M. GÓMEZ, L. RANCEL, S.F. MEDINA
"Effects of Nb, V, Ti and Al on recrystallisation/precipitation interaction in microalloyed steels"

Materials Science Forum
Vol. 638-642 (2010), Pages: 3388-3393
DOI: 10.4028/www.scientific.net/MSF.638-642.3388
ISSN: 0255-5476

Effects of Nb, V, Ti and Al on Recrystallisation/Precipitation Interaction in Microalloyed Steels

Manuel Gómez[1, a], Lucía Rancel[1, b] and Sebastián F. Medina[1, c]

[1] National Centre for Metallurgical Research (CENIM-CSIC), Av. Gregorio del Amo 8; 28040 Madrid, Spain

[a]mgomez@cenim.csic.es, [b]lucia.rancel@cenim.csic.es, [c]smedina@cenim.csic.es

Keywords: microalloyed steels, recrystallisation, precipitation, diffusion.

Abstract. Recrystallisation/precipitation interaction in four steels having Nb, V, Ti, and Al, respectively, as microalloying elements has been studied by means of hot torsion tests. Remarkable differences were found in the results obtained for each steel. Nb and V-microalloyed steels presented long inhibition plateaus, but the steel with Al displayed a very short plateau. Finally the steel with Ti did not show plateau. This means that Nb and V precipitates (nitrides and carbides) can inhibit the static recrystallization but this does not happen for Al and Ti (which form nitrides). The difference between activation energies allows to predict the efficiency of different precipitates to strengthen the austenite during hot rolling. RPTT diagrams showed the interaction between both phenomena, along with the strain induced precipitation kinetics and precipitate coarsening. It is found that AlN particles nucleate and grow faster than NbCN or VN.

Introduction

The type and amount of microalloying elements play an important role on the shape and the nature of precipitates. However, the impact of some elements that are not considered as authentic microalloying elements is usually underestimated, even though the influence of these elements on chemical composition, size and distribution of precipitates can be even stronger than that of microalloying. This is true for aluminium-killed, V-microalloyed steels, whose Al content is often higher than 0.020 mass%. VN particles are finer than AlN and therefore they have a stronger contribution during hot rolling [1]. Fine VN precipitates inhibit static recrystallisation of austenite, which leads to austenite strengthening during last hot rolling passes. Besides, VN promotes intragranular nucleation of ferrite. At equal level of Nb, Al, Ti or V alloying, the precipitates are soluble in austenite as follows [2]: TiN<AlN<NbN<VN. On the other hand the presence of AlN in the austenite generates harmful effects on the hot-ductility of different kinds of steels [3,4].

Crystallographic structure of AlN is hexagonal (h.c.p.). Nitrides and carbides of typical microalloying elements (Nb, V, Ti) have an f.c.c. crystallographic structure. These compounds, especially in the case of the smallest particles, frequently form precipitates which are semi-coherent with the (f.c.c) austenitic matrix. Their lattice parameter is slightly higher than that of the austenite [5].

In this work static recrystallisation of austenite is studied in four steels with different microalloying element. The influence of precipitates is studied and the convenience of restricting the Al content in microalloyed steels is established.

Materials and experimental procedure

Chemical compositions of steels used are shown in Table 1. The specimens for torsion testing had a gauge length of 50 mm and a diameter of 6 mm. The austenitisation temperature was set to be higher than the solubility temperature of precipitates, thus assuring that the precipitates would be completely dissolved in the austenite, except in Ti-steel. The mean austenite grain size corresponding to the austenitisation conditions was determined for each steel by applying ASTM E-112 standard (Table 2).

Table 1. Chemical composition of steel used [% mass x 10^3].

Steel	C	Mn	Si	Al	V	Nb	Ti	N
X3	94	1475	329	21	92	-	-	6.5
U11	90	1505	313	17	-	34	-	4.0
Y1	99	1463	297	37	-	-	-	10.0
S5	120	1180	290	34	-	-	18	8.0

Table 2**.** Austenite grain size ($\bar{d}$) for given reheating conditions.

Steel	Reheating conditions	($\bar{d}$), [μm]
X3	1200ºCx10min	151
U11	1200ºCx10min	107
Y1	1300ºCx10min	550
S5	1300ºCx10min	38

After austenitisation, the specimens were rapidly cooled to the deformation temperature in order to prevent precipitation prior to deformation. The deformation temperatures were between 1100ºC and 800ºC, and the recrystallised fraction (X_a) was determined for several holding times after deformation. The applied strains were 0.20 and 0.35, which were insufficient to promote dynamic recrystallisation [6]. The double deformation technique was used to calculate X_a, in particular applying the method known as "back extrapolation" [7].

Microstructures of the transformed specimens were examined by means of optical and transmission electron microscopy (TEM). For optical observations, specimens were etched with 2% nital. Carbon extraction replicas were used for precipitate analysis by TEM. Electron probe microanalyser (EPMA) and TEM-EDS (energy dispersive X-ray spectroscopy) analyses were made for identifying precipitate phases.

Results and discussion

The static recrystallisation kinetics of austenite can be described by an Avrami equation in the following way [8,9]:

$$X_a = 1 - \exp\left[-0.693\left(\frac{t}{t_{0.5}}\right)^n\right]. \quad (1)$$

where X_a is the fraction of the recrystallised volume and $t_{0.5}$ is the time corresponding to 50% recrystallisation, which depends practically on all the variables that intervene in hot deformation and whose most general expression can be defined by the equation:

$$t_{0.5} = A\varepsilon^p \dot{\varepsilon}^q D^s \exp\frac{Q_x}{RT}. \quad (2)$$

where ε is the strain, $\dot{\varepsilon}$ the strain rate, D the grain size, Q_x the activation energy, T the absolute temperature, R=8.3145 $Jmol^{-1}K^{-1}$, and *p, q* and *s* are parameters. While *p* and *q* are negative values, *s* is positive.

On the other hand, the activation energy (Q_x) for the static recrystallisation of austenite in the presence of precipitates may be expressed as the sum of two terms:

$$Q_x = Q + \Delta Q. \quad (3)$$

where Q represents the activation energy in the absence of precipitates and ΔQ represents the increase due to the presence of the precipitates. Precipitates in austenite produce a delaying effect on recrystallisation kinetics, due to the fact that the pinning forces –which try to prevent grain boundary self-diffusion– increase considerably.

The shape of the recrystallised fraction against time curves for the V and Nb microalloyed steels presented one and two plateaus, respectively, when the test temperatures were below those where the particles have precipitated. Fig. 1 shows the recrystallised fraction for steel X3 at a strain of 0.20, strain rate of 3.63 s^{-1} and several temperatures, with a plateau appearing on the curve corresponding at 900ºC and 850°C. Fig. 2 presents the recrystallised fraction kinetics for steel U11 at a strain equal to 0.35 showing two plateaus in the curves plotted at 1000 ºC and 950 ºC.

Regarding the steel with Al as microalloying element(Y1), recrystallised fraction (Fig. 3) was determined strain value of 0.20 and 0.35, respectively, and deformation temperature of 1000ºC. A very short plateau can be distinguished. Recrystallisation curves could have been assimilated to a sigmoidal regression, but previous studies carried out on steels where Al was the sole alloying element have confirmed that a small plateau -like that displayed in present study- appears as a result of AlN precipitation [1]. Fig. 4 corresponds to Ti-microalloyed steel (S5) where no plateau is observed, as the TiN particles were not put in solution at reheating temperature of 1300ºC.

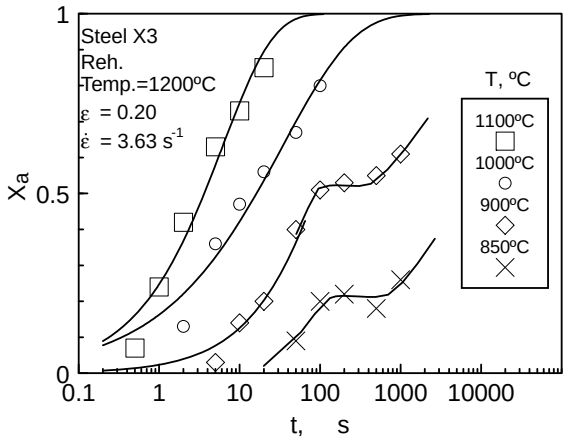

Fig. 1. Recrystallised fraction (X_a) vs. time (t) for steel X3.

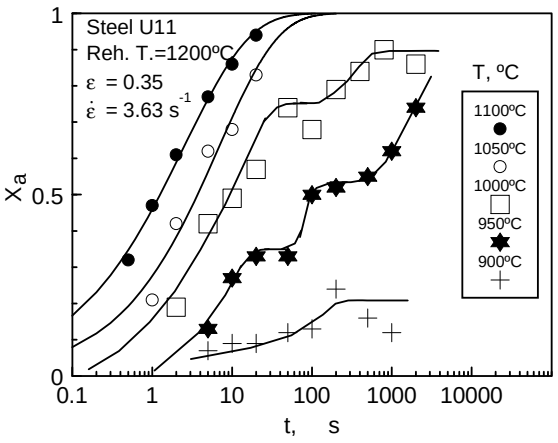

Fig. 2. Recrystallised fraction (X_a) vs. time (t) for steel U11.

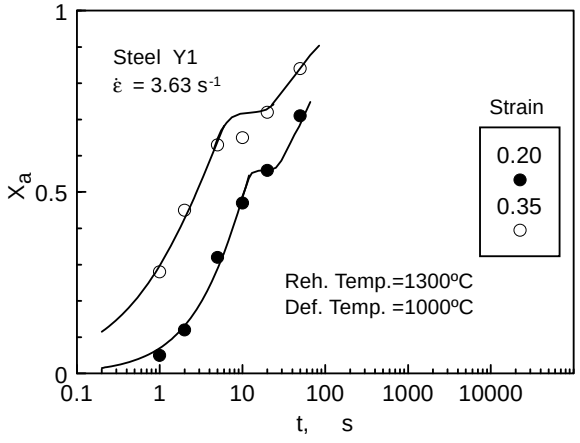

Fig. 3. Recrystallised fraction (X_a) v. time (t) for steel Y1.

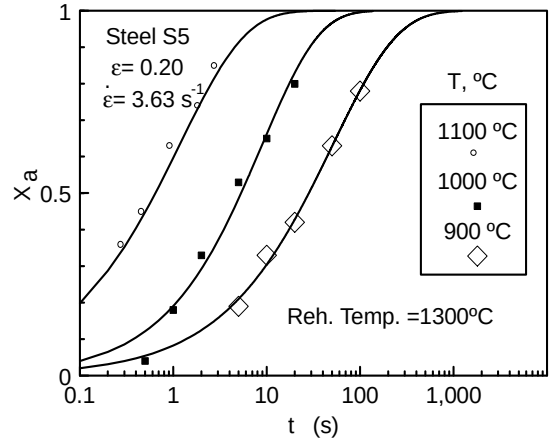

Fig. 4. Recrystallised fraction (X_a) v. time (t) for steel S5.

Figures showing the recrystallised fraction versus time were used to deduce the temperature and times corresponding to different recrystallised fractions. The points that define the start and the end of

the plateau were taken to plot the induced precipitation start (P_s) and finish (P_f) curves, respectively. In this way recrystallisation-precipitation-time-temperature (RPTT) diagrams for the studied steels were drawn. The recrystallised fraction does not vary between the precipitation start (P_s) and finish (P_f) curves and is represented by a horizontal line. Once the P_f curve is reached, the lines of each recrystallised fraction descend again (Fig. 5).

The values of the minimum incubation time (t_N) and the curve nose temperature (T_N) are shown in Table 3 for the steels studied. The value of t_N decreases as the strain increases. On the other hand, comparison of RPTT diagrams showed that AlN particles nucleate earlier and grow faster than VCN and NbCN particles.

With regard to the recrystallisation-precipitation interaction, it is seen that the nose of the P_s curve, where the incubation time of the precipitates (t_N) is the shortest, the recrystallised fraction is approximately 50%. When the fraction of recrystallised volume is less than 20%, nucleation of the precipitates needs longer time to take place.

The activation energy can be easily determined from recrystallised fraction against time curves or from RPTT diagrams. In accordance with Eq. (2), Fig. 6 displays the parameter $t_{0.5}$ against the inverse of the absolute temperature for steel X3 at two strains of 0.20 and 0.35. The line $ln\ t_{0.5}$ against $1/T$ shows a discontinuity just when the temperature reaches the nose of RPTT diagram. The value of the activation energy changes from one stage to another. After precipitation the activation energy increases significantly, which is obviously translated into greater difficulty for the austenite to recrystallise [10]. The figure shows the values of Q and $Q+\Delta Q$. The comparison of the values shown in Table 4 demonstrates that the contribution of precipitates to the increment in activation energy (ΔQ) is much higher for VCN and NbCN precipitates than for AlN and obviously than TiN.

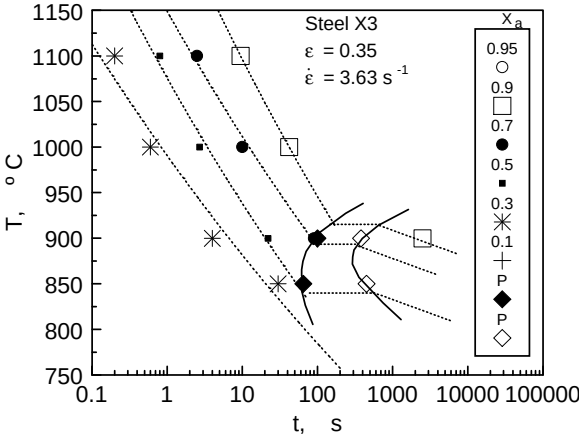

Fig. 5. RPTT diagram. Steel X3.

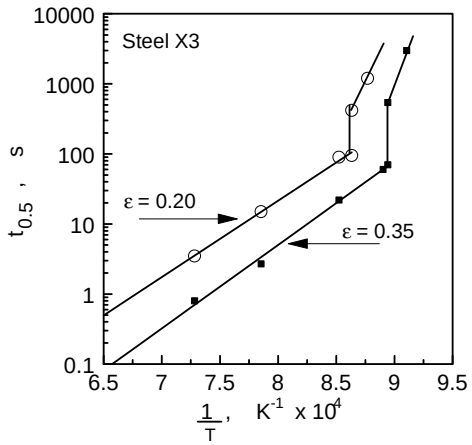

Fig. 6. Plot of $t_{0.5}$ against the reciprocal of the absolute temperature.

Table 3. T_N and t_N of the P_s curve nose;

Steel	ε	t_N, [s]	T_N, [ºC]
X3	0.20	95	887
X3	0.35	65	875
U11	0.20	70	975
U11	0.35	23	950
Y1	0.20	12	975
Y1	0.35	4	950

In order to know the type and size of the precipitates, a study was carried out, using transmission electron microscopy (TEM) techniques on carbon extraction replicas (Fig. 7). Prior to the simulation test the specimens were heated at reheating temperature. The temperature was then lowered to that corresponding to the nose temperature in RPTT diagram. The precipitation states

were characterized by studying the nature, size and distribution of nitrides-carbonitrides formed in hot-deformed specimens. The mean particle diameter has been obtained measuring an average number of two hundred particles on each specimen. Specimens were collected at the P_f curve, which coincides with end of the plateau on corresponding recristallised fraction vs time curve. The values found for the mean size are showed in the Table 5. The mean size for TiN particles in steel S5 corresponds to reheating temperature of 1300ºC, as RPTT diagram does not exist.

Table 4. Activation energy for static recrystallisation of the steels used.

Steel	Q [kJ]	Q+ΔQ [kJ]	ΔQ [kJ]
X3	215	510	295
U11	295	650	155
Y1	160	220	60
S5	220	220	0

Table 5. Mean size of precipitates.

Steel	Particle type	Mean size, [nm]
X3	VN	10.5
U11	NbCN	22
Y1	AlN	87
S5	TiN	1250

Mean size of VN and AlN particles was respectively equal to 10.5 nm and 87 nm, so the latter is almost one order of magnitude bigger than the former. For the calculation of pinning forces consideration was made of the expression of Gladman [5], which is proportional to reciprocal of precipitate size. That explains the formation of big plateau in steels X3 and U11, short plateau in steel Y1 and complete absence in steel S5.

On the other hand, the particle diameter at any temperature can be expressed as [11,12]:

$$\Delta d^2 = \alpha^2 D_0 \exp\left(-\frac{Q_d}{RT}\right)\Delta t \,. \tag{4}$$

Where, $D_0 \exp\left(-\frac{Q_d}{RT}\right)$ is the diffusion coefficient (D) of Al, V, Nb and N in austenite.

Eq. 4 can be applied to predict the growth of precipitates that nucleate during cooling. Regarding the coefficient D, it is represented in Fig. 8 for different elements [13]. The diffusion coefficient for Al is two orders of magnitude larger than for V. Besides, AlN particles start to precipitate at temperatures close to 1100ºC, while VN precipitation starts at much lower temperatures, near 950ºC [2]. This brings about an even more pronounced difference in parameter D in the first stages of precipitation. To sum up, the larger diffusion coefficient of Al compared to V and Nb, together with the higher precipitation temperature of AlN serve to explain the coarser size of AlN particles compared to VN and NbCN.

Conclusions

1. Inhibition of austenite recrystallization (plateau) is longer for V/Nb-microalloyed steels than for Al-steels, mainly due to their different precipitate sizes. This inhibition is not displayed in Ti-steels.
2. The mean size of strain-induced AlN precipitates is almost one order of magnitude bigger than the size of VCN particles.

3. The pinning forces exerted by coarse TiN precipitates are weak and accordingly the static recrystallisation of austenite is not inhibited by these particles. Pinning forces exerted by AlN are also weak and they are not sufficient to inhibit the recrystallisation of austenite.
4. Microalloyed steels should have a very low Al content. In this way, Al would not trap part of the N and the precipitated volume of VN or NbCN would be significantly higher. This would augment pinning forces and would contribute to a more intense strengthening of the austenite during rolling.
5. The larger diffusion coefficient of Al compared to V and Nb, together with the higher precipitation temperature of AlN serve to explain the coarser size of AlN particles compared to VN and NbCN.

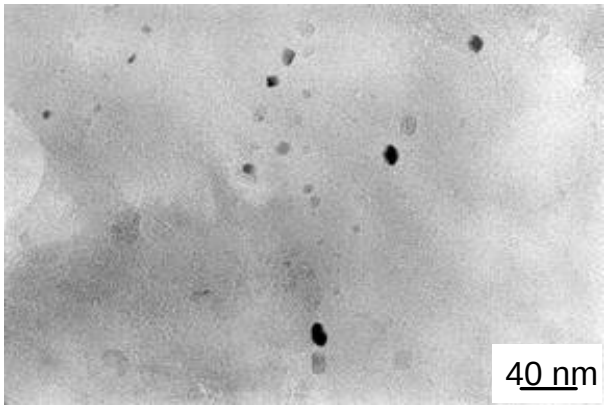

Fig. 7. TEM image of fine VN precipitates. Steel X3.

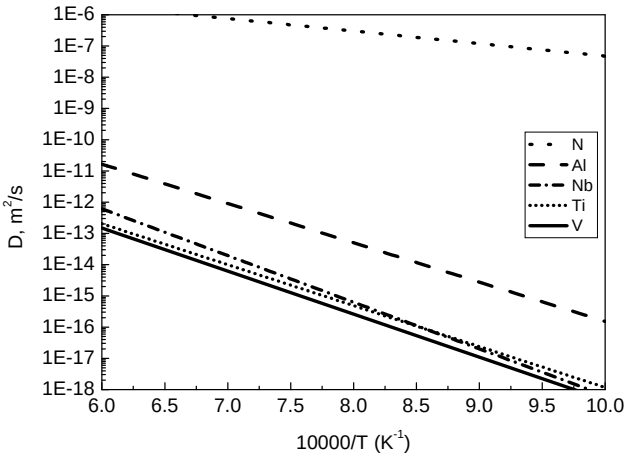

Fig. 8. Diffusion coefficient for Al, Nb, Ti, V and N.

References

[1] M. Gómez, L. Rancel, S.F. Medina: Mater. Sci. Eng. A, vol. 506 (2009), p. 165.

[2] E.T. Turkdogan: Iron Steelmaker vol. 3 (1989), p. 61.

[3] B. Mintz, J.M. Arrowsmith, in: C.M Sellars and G.J. Davies (ed), *Proc. Int. Conf. on Hot Working and Forming Processes*, Metal Society, London, (1980), p. 99.

[4] G.D. Funnell, in: C.M Sellars and G.J. Davies (ed), *Proc. Int. Conf. on Hot Working and Forming Processes*, Metal Society, London , (1980), p. 104.

[5] T. Gladman: *The Physical Metallurgy of Microalloyed Steels*, The Institute of Materials, London, (1997).

[6] S.F. Medina, C.A. Hernández: Acta Mater. 44 (1996), p. 149.

[7] J.S. Perttula, L.P. Karjalainem: Mater. Sci. Technol. 14 (1998), p. 626.

[8] S.F. Medina, A. Quispe, M. Gómez: Mater. Sci. Technol**.** 17 (2001), p. 536.

[9] J.H. Beynon, C.M. Sellars: ISIJ Int. 32 (1992), p. 359.

[10] A. Quispe, S.F. Medina, P. Valles: ISIJ Int. 37 (1997), p. 783.

[11] S.H. Park, S. Yue, J.J. Jonas: Metall. Trans A 23A (1992), p. 1641.

[12] S. Okaguchi, T. Hashimoto: ISIJ Int., 32 (1992), p. 283.

[13] A. Vignes, J. Philebert, J. Badía, J. Lavasseur: *Proc. 2nd Natl. Conf. Microprobe Analysis*, Boston, (1967), Paper 20.